

WUW_ · g | XY · f YWc aV | lh | c b j Y ·
 g \ i b h · f Yg | g h Ub WY gO) Q Ub X h
 WY · · Đg · YZZ | W | Yb Wm 7 c b g | XY
 c Z · a U [b Yh | W · Ub X · YWhf | WZ |
 Y · YWhf | WU · · dUf · Uaf YWf g Uf
 = b · O' Qž · U i h \ c f g · YX h \ Y W
 Wc b W i XYX · h \ Uh · h \ g c · Uf WY ·
 Ug · U · d · Ub Y · WUd UW · f k | h \ h
 g Yd Uf Uh YX · Vm · Ub · Y Yb g | d Yb Xg
 h \ Y · Xmb Ua | W · ^ i b Wh · b j Y · c W |
 V c i b X U f m · f YWc a V | b h | c b j Y ·
 g h i X mž · h \ Y · d f | a U f f c · Y c Z G
 d c | b h · c Z · h \ Y · g c · Uf · WY · ·] g
 < c k Y j Y f ž · h \ d Y f W U W a b Z U h \ Y |
 WY · · k \ | W \ [] j Y g · c X f Y g i · h
 h \ Y · W \ Uf U Wh Y f | n U h c b Ub X a i
 c f | Y b h Uh | c b · WUb · Ug c V Y Wc b |
 h \ Y · Wc b h f c · · c Z · h \ U Y · d Uf U a Y h

g h f c b [· ž · XH d | Y X Y Wc b X · ^ i b W
 j Y f m · | b h Y b g Y · Y Wh f | WZ | Y · X
 h c k U f X g · h) Q " V U g Y Y W d f | WU · · Z | Y ·
 f Y Wc a V | b U h | c b U h h \ Y V U W _ g
 k \ | W \ · U f Y · a c f Y Z Z | W | Y b h h \ !
) Q " ·
 5 W W c f X | b [· h c · % \$ Q ž h \ Y h f U t
 h \ Y · g c · Uf · WY · Uf Y a c Wc b h | b i | h m ·
 W m b | b X f | WU · · Wc c f X | b U h Y g ·

$$\frac{\partial^2 \psi}{\partial x^2} + \frac{\partial^2 \psi}{\partial y^2} + \frac{\partial^2 \psi}{\partial z^2} + \frac{\partial^2 \psi}{\partial t^2} = -\frac{e}{\hbar^2} \psi$$

5 g ž · k Y · \ U j Y · Un | a i h \ U · g
 d f g W c g h X Y · H c Y f Y Z c f Y h \ Y

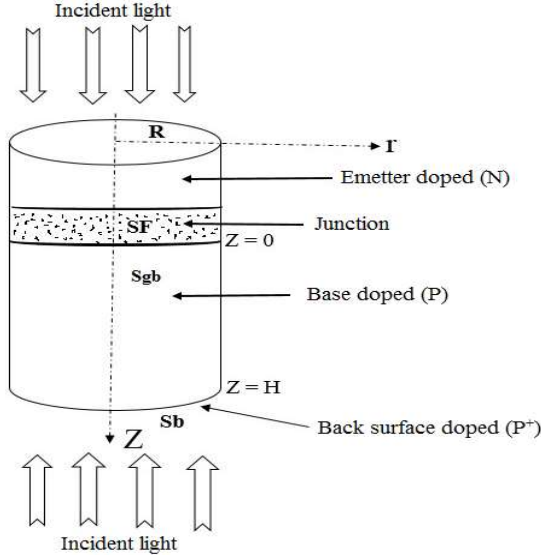
H \ Uh ·] g · k \ mž · h \ | g | d Y f U | a g
 h \ Y · h f Ub g | Y b h · X | ž i g D ! ž D V | Z U
 g c · Uf · WY · · " · H \ Y · V U W | h Ub W
 c f | Y b h Uh | c b · c Z · h \ [f U] b g c
 U W W c i Z b h \ Y · Xmb Ua | · i b Wh | c b
 f U X | i g · f F L · Ub X · h \ f U | b V c i
 f G [V L " ·

$$\frac{\partial^2 \psi}{\partial x^2} + \frac{\partial^2 \psi}{\partial y^2} + \frac{\partial^2 \psi}{\partial z^2} = -\frac{E}{\hbar^2} \psi$$

đ f f / n L · · a | b d f g | h m · W U f f | Y f Đ g · X
 8 · Y · Y W h f c b · X | ž i g | c b Wc Y Z ·
 g L / ·
 @ · Y · Y W h f c b · X Z ž i g ·
 ; f n L a | b c f | h m · U f f | Y f g [Y b Y
 V U g Y · O' Q ·
 K \] · Y · d f c W Y Y | b [V m h \ Y g Y d |
 i g Y X · V m · O % \$ Q ž · k Y · d i h ·

&" H \ Y c f m

K Y · d f Y g Y b h ·] b · Z | [Y % Ub] g ·
 V | Z U W | U · · g | ·] Wc b · · Uf WY · ·



$$\delta = \sum_{z=0}^{\infty} \dots$$

$$\delta = \sum_{z=0}^{\infty} \left[\frac{5f + \frac{\alpha \cdot \dots}{8} \frac{W}{W + \alpha} \dots}{\dots} \right]$$

7 c Y Z Z | W | Y b X g · U f Y · Y X · Z f c a · h \ Y ·
 V c i b X U f h | Y g b W c Z X | ·
 • 5 h · h \ Y · ^ i W h |

$$\frac{\partial \delta}{\partial n} \Big|_{nS} = \frac{G \cdot Z}{8} \cdot \delta = \dots$$

$$\frac{\partial}{\partial f} \dots = -\frac{G [V]}{8} \dots$$

' " 7 U d U W | h U b W Y

: | [i f g c % Uh Y X · W m ·] b X f | W U · · [f U] b V | Z U W | U · · c · Uf WY · · Đ g f

H \ Y · V | Z U W | U · · g c · U W Y · ·] g U
 Y a | h h Y f ž X h d Y X V B g Y c d Y X ž · k \ | W \ ·
] g · g W Y h h Y X Y b · h \ Y · Y | h h Y f U b |
 Wc b h U Wh · k \ Y f Y · Ub c \ Y f ^ i b W

$$\frac{G \cdot Z \cdot e}{J_H} \left[\frac{\delta \dots}{B_V} \right] \dots$$



A method to determine the transient capacitance of the bifacial solar cell considering the cylindrical model of the grain and the dynamic junction velocity (SF)

4. Results and Discussions

In figures 2, 3 and 4, we plotted the transient diffusion capacitance versus the junction recombination velocity. Figure 2 shows effects of grain boundary recombination velocity. As for the influence of the grain size and wavelength (λ), we considered various radius (R) and wavelength (λ) in figures 4 and 5, respectively.

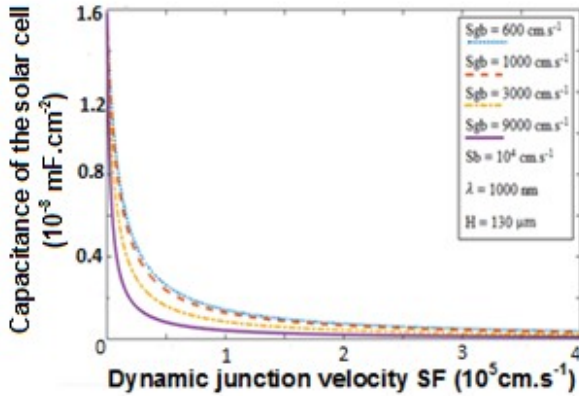


Figure 2. Capacitance of the illuminated solar cell versus SF for various Sgb: R= 0.01 cm.

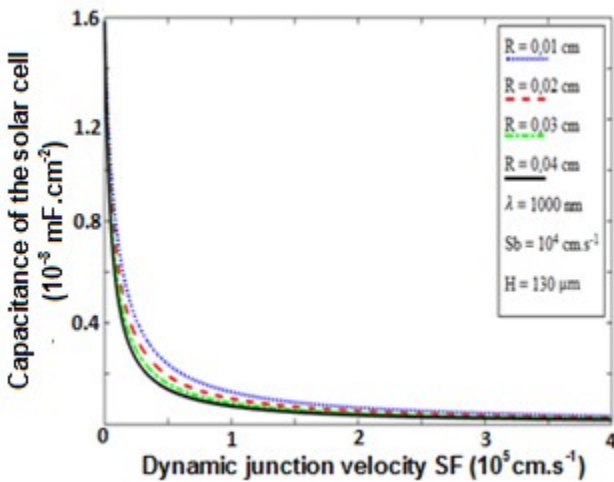


Figure 3. Capacitance of the illuminated solar cell by the front surface versus SF for various radius (R): L = 0.01 cm

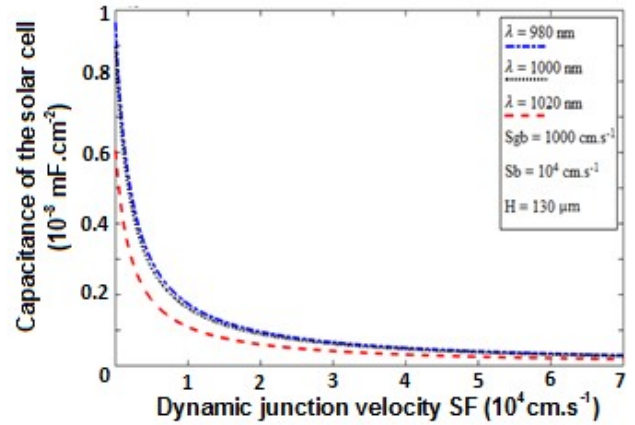


Figure 4. Capacitance of the illuminated solar cell versus SF for various wavelength: L = 0.01 cm and R= 0.01 cm

We remarked in figure 2, for a given solar cell, that:

- the open circuit transient diffusion capacitance is very brief. It can be seen here that there is a difference between the considered model and that of the cubic grains where the range of operating points of the open circuits is sufficiently long [4].
- the short circuit operating points zone is very important and there, the transient diffusion capacitance stretches toward zero ;
- a transient diffusion capacitance, depending on operating point which is related to SF, appears between the open circuit operating to the short – circuit operating points.

The increase of SF corresponds to an increase of the extension region width and hence to the increase of solar cell's photocurrent as shown by [3].

We also noted that the transient diffusion capacitance decreases with Sgb; meaning that increasing of Sgb leads to high recombination in the grain boundary of the solar. In figure 3, we noticed that the variation of the solar cell grain radius (R) leads to increase the transient diffusion capacitances.

Figure 4 shows that when the wavelength (λ) increases in the considered range between 980 to 1020 nm, the transient diffusion capacitance decreases. When the wavelength increases, the energy of incoming photons decreases and less excess minority carriers are extracted in the base of the solar cell.

In figure 5 we represented the solar cell's transient diffusion capacitance versus the dynamic junction velocity (SF) and the solar cell grain radius (R). Indeed, the solar cell's capacitance increases according to the grain radius (R) and decreases with the junction recombination velocity.

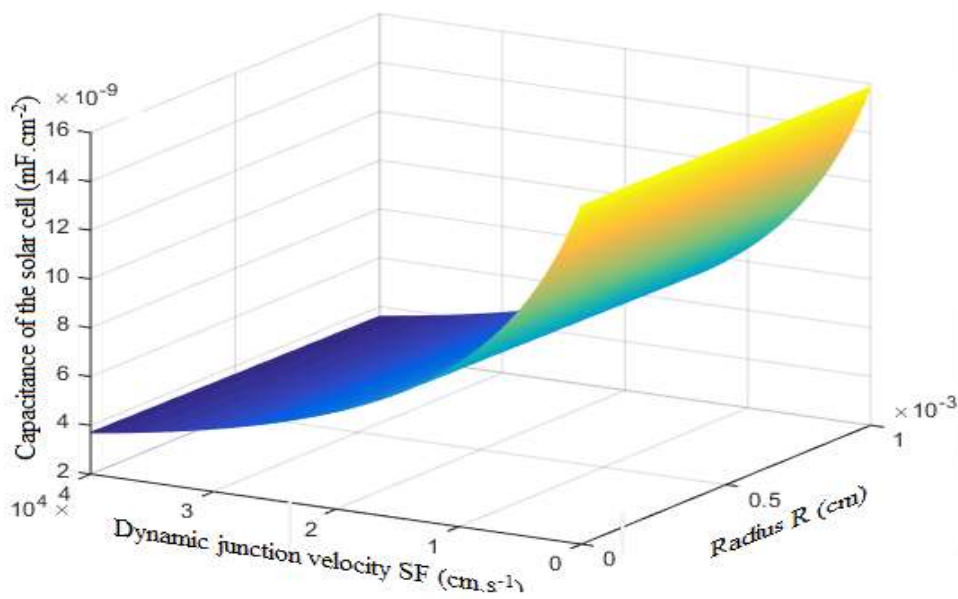


Figure 5. Capacitance of the illuminated solar cell by the front side versus SF and solar cell grain radius (R): $\lambda=1000$ nm, $S_{gb}= 1000$ cm.s⁻¹, $S_b = 10000$ cm.s⁻¹, $L = 0.01$ cm and $H=130$ μ m.

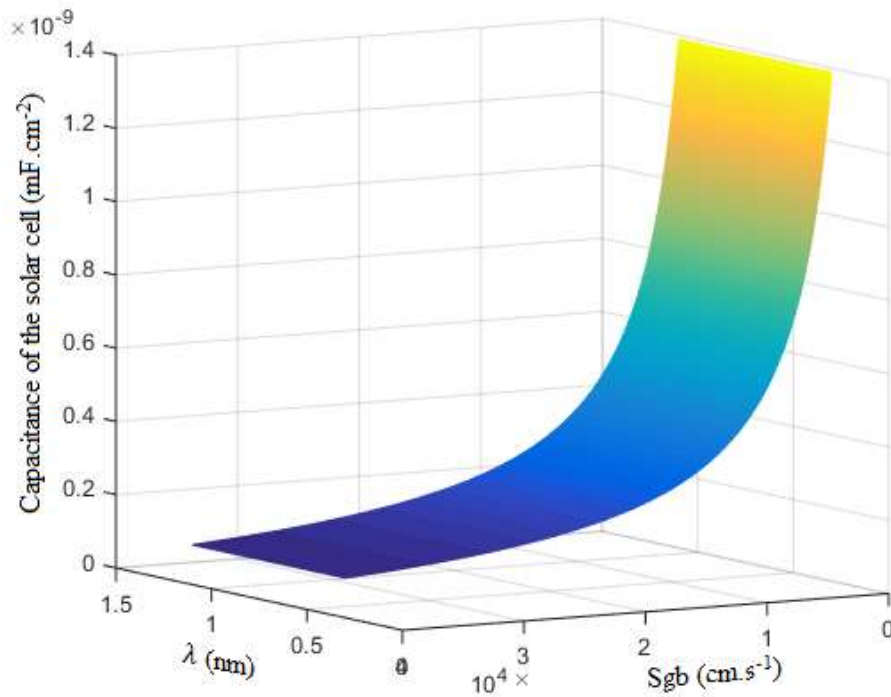


Figure 6. Capacitance of the illuminated solar cell by the front surface according to the grain boundary recombination velocity (S_{gb}) and wavelength (λ): $S_b = 10^4$ cm.s⁻¹, $L = 0.01$ cm, $H=130$ μ m and $R = 0.01$ cm

In figure 6, we showed the variation of the capacitance according to Sgb and the wavelength (λ). These figures represent the bifacial solar cells transient diffusion capacitance for a fixed solar cell grain radius (R) and for various grain boundary recombination velocities (Sgb) and wavelengths (λ). Effects of these two parameters on the transient diffusion capacitance are the same as for the results of [3].

5. Conclusion

In this paper, we determined the transient diffusion capacitance using the cylindrical orientation of solar cell's grains. We have shown that, as for the columnar isolated grain model, the diffusion transient diffusion capacitance increases with solar cell grain radius (R) and with wavelength. It decreases with the grain boundary recombination velocity and the dynamic junction velocity (SF). The approach confirms that best solar cells correspond to high grain radiuses (R) which lead to low grain boundary recombination velocity (Sgb).

Acknowledgements.

The authors would like to thank Alioune DIOP University of Bambey which sponsored this work.

References

- [1] Barro, F.I., Mbodji, S., Ndiaye, M., Maiga, A.S. and Sissoko, G.: (2008) Bulk and surface recombination parameters measurement of silicon solar cell under constant white bias light. *Journal des Sciences/ J. Sci.*, **8**, (4): pp. 37-41.
- [2] Barro, F.I., Mbodji, S., Ndiaye, A.L., Zerbo, I., Madougou, S., Zougmore, F. and Sissoko, G.: (7-11 June 2004) Bulk and surface parameters determination by a transient study of bifacial silicon solar cell under constant white bias light. *Proceedings of 19th European Photovoltaic Solar Energy Conference*, Paris, France: pp. 262-265
- [3] Mbodji, S., Mbow, B., Barro, F. I. and Sissoko, G.: (2011) A 3D model for thickness and diffusion capacitance of emitter base junction determination in a bifacial polycrystalline solar cell under real operating condition. *Turkish Journal of Physics*, **15**, Issue 3: pp. 281-291
- [4] Mbodji, S., Dieng, B., Mbow, M.B., Barro, F.I. and Sissoko, G.: (2010) Three dimensional simulated modelling of diffusion capacitance of polycrystalline bifacial silicon solar cell. *Journal of Applied Science and Technology (JAST)*, **15**, Nos. 1 & 2: pp. 109-114.
- [5] Mbodji, S. and Sissoko, G.: (2011) A method to determine the solar cell resistances from single I-V characteristic curve considering the Junction recombination velocity (Sf). *Int. J. Pure Appl. Sci. Technol.*, **6**(2) : pp.103-114
- [6] Sissoko, G., Museruka, C., Corréa, A., Gaye, I. and Ndiaye, A.L. (1996) Light Spectral Effect on Recombination Parameters of Silicon Solar Cell. *World Renewable Energy Congress*, **III** : pp. 1487-1490
- [7] Ly, I., Wade M., DIALLO, H.L., EL Moujtaba, M.A.O., Lemrabott, O.H., Mbodji, S., Diasse, O., Ndiaye, A., Gaye, I., Barro, F.I., Wereme, A. and Sissoko, G. (2011) Irradiation effect on the electrical parameters of a bifacial silicon solar cell under multispectral illumination. *Proceedings of 26th European Photovoltaic Solar Energy Conference and Exhibition*: pp. 785-788
- [8] Madougou, S., Made, F., Boukary, M. S. and Sissoko, G. (2007) I-V Characteristics for bifacial silicon solar cell studied under a magnetic field, *Advanced Materials Research*, **18** (19) : pp. 303-312
- [9] Mbodji, S., Zoungrana, M., Zerbo, I., Dieng, B. and Sissoko, G. (2015) Modelling Study of Magnetic Field's Effects on Solar Cell's Transient Decay. *World Journal of Condensed Matter Physics*, **5** : pp. 284-293.
- [10] Trabelsi, A., Zouari, A. and Ben Arab, A. (2009) Modeling of polycrystalline N⁺/P junction solar cell with columnar cylindrical grain. *Revue des Energies Renouvelables*, **12**, N°2 : pp. 279-297